Available online at www.sciencedirect.com
ScienceDirect
Journal of Sound and Vibration 315 (2008) 1035–1046
JOURNAL OF SOUND AND VIBRATION
www.elsevier.com/locate/jsvi

The effect of static loading and imperfections on the nonlinear vibrations of laminated cylindrical shells

E.L. Jansen*

Faculty of Aerospace Engineering, Delft University of Technology, Kluyverweg 1, 2629 HS Delft, The Netherlands

Received 21 May 2007; received in revised form 5 February 2008; accepted 6 February 2008
Handling Editor: C.L. Morfey
Available online 18 April 2008

Abstract

The effect of static loading and imperfections on the nonlinear vibration behaviour of cylindrical shells is studied. The two analytical–numerical models (denoted as Level-1 and Level-2 Analysis) that are used for this purpose are based on Donnell-type governing equations and have different levels of complexity. Parametric studies have been performed for a specific laminated shell. The axial compressive loading and different imperfection shapes can significantly influence the linearized vibration behaviour and also affect the nonlinear vibration behaviour. Results show that certain axisymmetric imperfections, satisfying a strong-coupling condition with the asymmetric vibration mode, reduce the linearized vibration frequencies and make the nonlinearity less softening, while the static compressive axial loading makes the nonlinearity more softening.

1. Introduction

Shell structures are widely used in mechanical and aerospace engineering. It is well known that these thin-walled structures are prone to buckling instabilities under static and dynamic compressive loading. Moreover, they may be directly or parametrically excited into resonance at their natural frequencies by dynamic loads, and they may experience flutter in a flow.

The important problem of the nonlinear vibration behaviour of cylindrical shells has been studied since the beginning of the space age (about 1960). Traditionally, investigations of nonlinear vibrations of cylindrical shells have been analysed using analytical–numerical approaches. The spatial dependence was very often taken care of by means of a Galerkin-type discretization (e.g. Refs. [1,2]) or via an analytical approach (e.g. Refs. [3,4]). During the mid-1990s a finite element approach was presented by Ganapathi and Varadan [5,6].

The topic has received a considerable amount of attention to date, and several important effects are understood reasonably well, including ''secondary'' modes (axisymmetric modes and modes with the double number of full waves in the circumferential direction of the shell) and modal interactions [1,3,4,7–9]. Pellicano et al. [8] presented multimode Galerkin-type solutions for simply supported boundary conditions. The effect of

*Tel.: +31 15 27 82592; fax: +31 15 27 85337.
E-mail address: e.l.jansen@tudelft.nl

0022-460X/$ - see front matter © 2008 Elsevier Ltd. All rights reserved.
doi:10.1016/j.jsv.2008.02.004

imperfections was included by Amabili in Ref. [10]. Amabili [11] also investigated the effect of different boundary conditions. An extensive review on nonlinear vibrations of circular cylindrical shells can be found in Ref. [12].

In Ref. [9] several analytical–numerical models with different levels of accuracy and complexity (denoted as Level-1 and Level-2 Analysis) have been presented which can be used to study the influence of important parameters on shell vibrations, such as geometric imperfections, static loading (axial compression, radial pressure and torsion) and boundary conditions. Nonlinear Donnell-type governing equations are adopted in combination with classical lamination theory. In Ref. [9], these models have been compared for the nonlinear vibration analysis of isotropic and orthotropic shells. In Ref. [13] laminated shells were studied, while in Ref. [14] the effect of imperfections on the linearized vibrations of shells was investigated, and in Ref. [15] the effect of boundary conditions on the nonlinear vibrations.

In his review on the early developments in the field of nonlinear vibrations of shells [16], Evensen already remarked that the effect of static loading can make the nonlinear effects much more pronounced. However, the effect of static loading on nonlinear shell vibrations did not yet receive much attention in the literature. The aim of the present work is to investigate the effects of axial compression and imperfections on the nonlinear vibration behaviour of cylindrical shells. In particular, the behaviour of a laminated shell earlier used in static and vibration analyses [13–15] will be studied in the present paper. In the next sections, the underlying theory and analysis models earlier described in Ref. [9] will first be recapitulated.

2. Governing equations

The shell geometry and the applied loading are defined in Fig. 1. The shell geometry is characterized by its length L, radius R and thickness h. Assuming that the radial displacement W is positive inward (see Fig. 1) and introducing an Airy stress function F as $N_x = F_{,yy}$, $N_y = F_{,xx}$ and $N_{xy} = -F_{,xy}$, where N_x, N_y and N_{xy} are the usual stress resultants, then the Donnell-type nonlinear imperfect shell equations (neglecting in-plane inertia) for a general anisotropic material can be written as

$$L_{A^*}(F) - L_{B^*}(W) = -\frac{1}{R}W_{,xx} - \frac{1}{2}L_{NL}(W, W + 2\bar{W}) \tag{1}$$

$$L_{B^*}(F) + L_{D^*}(W) = \frac{1}{R}F_{,xx} + L_{NL}(F, W + \bar{W}) + p - \bar{\rho}hW_{,tt} \tag{2}$$

where the variables W and F depend on the time t, R is the shell radius, $\bar{W}$ is an initial radial imperfection, $\bar{\rho}$ is the (averaged) specific mass of the laminate, h is the (reference) shell thickness, p is the (effective) radial

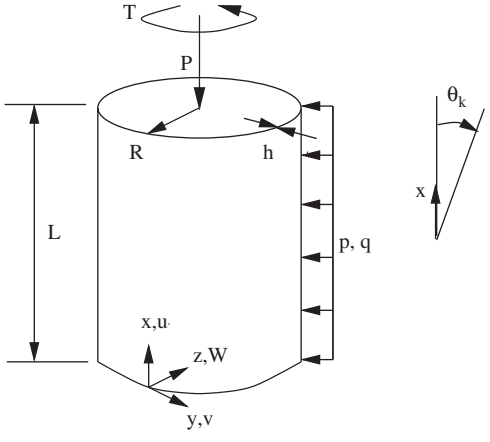

Fig. 1. Shell geometry, coordinate system and applied loading.

pressure (positive inward), and $\bar{\rho}hW_{,tt}$ is the radial inertia term. The fourth-order linear differential operators

$$L_{A^*}() = A^*_{22}()_{,xxxx} - 2A^*_{26}()_{,xxxy} + (2A^*_{12} + A^*_{66})()_{,xxyy} - 2A^*_{16}()_{,xyyy} + A^*_{11}()_{,yyyy} \tag{3}$$

$$L_{B^*}() = B^*_{21}()_{,xxxx} + (2B^*_{26} - B^*_{61})()_{,xxxy} + (B^*_{11} + B^*_{22} - 2B^*_{66})()_{,xxyy} + (2B^*_{16} - B^*_{62})()_{,xyyy} + B^*_{12}()_{,yyyy} \tag{4}$$

$$L_{D^*}() = D^*_{11}()_{,xxxx} + 4D^*_{16}()_{,xxxy} + 2(D^*_{12} + 2D^*_{66})()_{,xxyy} + 4D^*_{26}()_{,xyyy} + D^*_{22}()_{,yyyy} \tag{5}$$

depend on the stiffness properties of the laminate. The stiffness parameters A^*_{ij}, B^*_{ij}, and D^*_{ij} are coefficients of the partially inverted ABD-matrix from classical lamination theory and can be found in Ref. [9]. The nonlinear operator defined by

$$L_{NL}(S,T) = S_{,xx}T_{,yy} - 2S_{,xy}T_{,xy} + S_{,yy}T_{,xx} \tag{6}$$

reflects the geometric nonlinearity.

The shell can be loaded by axial compression P, radial pressure p and counter-clockwise torsion T (Fig. 1), both statically ($\tilde{P}$, $\tilde{p}$, $\tilde{T}$) and dynamically ($\hat{P}$, $\hat{p}$, $\hat{T}$). The equations governing the nonlinear dynamic behaviour of a cylindrical shell vibrating about a nonlinear static state will be derived, by expressing both the displacement W and the stress function F as a superposition of two states

$$W = \tilde{W} + \hat{W} \tag{7}$$

$$F = \tilde{F} + \hat{F} \tag{8}$$

where $\tilde{W}$ and $\tilde{F}$ are the radial displacement and stress function of the static, geometrically nonlinear state which develops under the application of a static load on the imperfect shell, while $\hat{W}$ and $\hat{F}$ are the radial displacement and stress function of the dynamic state corresponding to the large amplitude vibration about the static state.

The Donnell-type equations governing the nonlinear dynamic state can be written as

$$L_{A^*}(\hat{F}) - L_{B^*}(\hat{W}) = -\frac{1}{R}\hat{W}_{,xx} - \frac{1}{2}L_{NL}(\tilde{W},\hat{W}) - \frac{1}{2}L_{NL}(\hat{W},\tilde{W}+2\bar{W}) - \frac{1}{2}L_{NL}(\hat{W},\hat{W}) \tag{9}$$

$$L_{B^*}(\hat{F}) + L_{D^*}(\hat{W}) = \frac{1}{R}\hat{F}_{,xx} + L_{NL}(\tilde{F},\hat{W}) + L_{NL}(\hat{F},\tilde{W}+\bar{W}) + L_{NL}(\hat{F},\hat{W}) + \hat{p} - \bar{\rho}h\hat{W}_{,tt} \tag{10}$$

where $\hat{p}$ is the dynamic radial loading. It is noted that the coefficients of the dynamic state equations depend on the solution of the static state problem.

The Donnell-type equations for the nonlinear dynamic state of a perfect shell can be deduced from Eqs. (9) and (10) [9].

3. Simplified Analysis

At the modelling level denoted as Level-1 Analysis or Simplified Analysis, the vibration behaviour is modelled via a Galerkin procedure or variational method. The Level-1 model that will be used to investigate the nonlinear vibrations of statically loaded, imperfect laminated (anisotropic) cylindrical shells is characterized by the following deflection function:

$$\hat{W}(t)/h = \frac{\ell^2}{4R}\left[A(t)\sin\frac{m\pi x}{L}\right]^2 + A(t)\sin\frac{m\pi x}{L}\cos\frac{\ell}{R}(y - \tau_K x) \tag{11}$$

where m denotes the number of half waves in the axial direction, ℓ is the number of full waves in the circumferential direction, and τ_K is a skewedness parameter, introduced to account for a possible skewedness of the asymmetric modes. The expression contains one generalized coordinate, $A(t)$, the amplitude of the ''primary'', ''driven'' mode. The corresponding model will be referred to as Evensen's approach [1]. Galerkin's procedure is applied in order to eliminate the spatial dependence. Using Eq. (11), and applying the method of averaging to eliminate the time dependence, results in a nonlinear equation for the average vibration amplitude $\bar{A}$

$$(a_{10} - \alpha_{10}\Omega^2)\bar{A} + (a_{31} - \alpha_{31}\Omega^2)\bar{A}^3 + a_{50}\bar{A}^5 = G_{m\ell\tau} \tag{12}$$

where a_{ij} and α_{ij} are constant coefficients depending on the shell properties, imperfection, vibration mode, and applied loading, and where $G_{m\ell\tau}$ is the generalized dynamic excitation. The coefficients are listed in Ref. [17]. The normalized frequency parameter Ω is defined by $\Omega = \omega/\omega_{\text{lin}}$, where $\omega_{\text{lin}} = \sqrt{a_{10}/\alpha_{10}}$ is the small amplitude (''linearized'') frequency for the given parameters. Eq. (12) can be used to calculate amplitude–frequency curves for nonlinear single-mode free or forced vibrations of statically loaded, imperfect anisotropic cylindrical shells.

4. Extended Analysis

At the second level of modelling, Level-2 Analysis (Extended Analysis), the boundary conditions at the shell edges can be taken into account accurately [13,15]. A Fourier decomposition of the solution is used in the circumferential direction of the shell, in order to eliminate the dependence on the circumferential coordinate. Subsequently, the resulting boundary value problem for ordinary differential equations in the axial direction is solved numerically by means of the parallel shooting method [18]. A perturbation method is used to assess the influence of large vibration amplitudes, geometric imperfections, and a static deformation on the vibration behaviour [19,20].

4.1. Perturbation expansion

For the static state the following perturbation expansion is assumed:

$$\tilde{W} = \tilde{W}^{(0)} + \xi_s \tilde{W}^{(1)} + \xi_s^2 \tilde{W}^{(2)} + \cdots \tag{13}$$

$$\tilde{F} = \tilde{F}^{(0)} + \xi_s \tilde{F}^{(1)} + \xi_s^2 \tilde{F}^{(2)} + \cdots \tag{14}$$

where ξ_s is a measure of the displacement amplitude of the static ''asymmetric'' (non-axisymmetric) mode. In the case of free vibrations, the dynamic lateral excitation is equal to zero ($\hat{p} = 0$). Considering the case of ''single mode'' vibrations, i.e. that a single ''primary'' vibration mode is associated with the (linear) natural frequency ω_c, the following perturbation expansion for the frequency ω is used,

$$\left(\frac{\omega}{\omega_c}\right)^2 = 1 + a_d\xi_v + b_d\xi_v^2 + \cdots + (b_{110}\xi_t + b_{101}\bar{\xi}) + (b_{210}\xi_t + b_{201}\bar{\xi})\xi_v + \cdots + (b_{120}\xi_t^2 + b_{111}\xi_t\bar{\xi} + b_{102}\bar{\xi}^2) + \cdots \tag{15}$$

and the corresponding solution is assumed as

$$\hat{W} = \xi_v \hat{W}^{(1)} + \xi_v^2 \hat{W}^{(2)} + \cdots + \xi_t\xi_v \hat{W}^{(11)} + \xi_t\xi_v^2 \hat{W}^{(12)} + \cdots + \xi_t^2\xi_v \hat{W}^{(21)} + \xi_t^2\xi_v^2 \hat{W}^{(22)} + \cdots + \cdots \tag{16}$$

$$\hat{F} = \xi_v \hat{F}^{(1)} + \xi_v^2 \hat{F}^{(2)} + \cdots + \xi_t\xi_v \hat{F}^{(11)} + \xi_t\xi_v^2 \hat{F}^{(12)} + \cdots + \xi_t^2\xi_v \hat{F}^{(21)} + \xi_t^2\xi_v^2 \hat{F}^{(22)} + \cdots + \cdots . \tag{17}$$

In these expansions $\xi_t = \xi_s + \bar{\xi}$, where $\bar{\xi}$ is the amplitude of an ''asymmetric'' imperfection, and ξ_v is a measure of the displacement amplitude; $\hat{W}^{(1)}$ will be normalized with respect to the shell thickness h and $\hat{W}^{(2)}$ is orthogonal to $\hat{W}^{(1)}$ in an appropriate sense [17]. A formal substitution of these expansions into the nonlinear governing equations for the perfect shell yields a sequence of equations for the functions appearing in the expansions.

4.2. First-order state

The equations governing the first-order dynamic state are given by

$$L_{A^*}(\hat{F}^{(1)}) - L_{B^*}(\hat{W}^{(1)}) = -\frac{1}{R}\hat{W}_{,xx}^{(1)} - \hat{W}_{,yy}^{(1)}(\tilde{W}_{,xx}^{(0)} + h\bar{w}_{0,xx}) \tag{18}$$

$$L_{B^*}(\hat{F}^{(1)}) + L_{D^*}(\hat{W}^{(1)}) = \frac{1}{R}\hat{F}_{,xx}^{(1)} + \tilde{F}_{,xx}^{(0)}\hat{W}_{,yy}^{(1)} - 2\tilde{F}_{,xy}^{(0)}\hat{W}_{,xy}^{(1)} + \tilde{F}_{,yy}^{(0)}\hat{W}_{,xx}^{(1)} + \hat{F}_{,yy}^{(1)}(\tilde{W}_{,xx}^{(0)} + h\bar{w}_{0,xx}) + \hat{p} - \bar{\rho}h\hat{W}_{,tt}^{(1)}. \tag{19}$$

Note that the coefficients of these equations depend on the solution of the fundamental state problem $(\tilde{W}^{(0)}, \tilde{F}^{(0)})$ and initial axisymmetric imperfection $\bar{W} = h\bar{w}_0(x)$. The corresponding equations for the static first-order state $(\tilde{W}^{(1)}, \tilde{F}^{(1)})$ are similar, but do not include the inertia term. The dynamic first-order state equations admit separable solutions of the form

$$\hat{W}^{(1)} = h\{\hat{w}_1(x)\cos n\theta + \hat{w}_2(x)\sin n\theta\}\cos\omega t \tag{20}$$

$$\hat{F}^{(1)} = \frac{ERh^2}{c}\{\hat{f}_1(x)\cos n\theta + \hat{f}_2(x)\sin n\theta\}\cos\omega t \tag{21}$$

where $\theta = y/R$, and n is the number of circumferential waves.

4.3. Second-order states

To determine the initial nonlinearity of the large amplitude vibrations, the equations of the dynamic second-order state (ξ_v^2-terms) have to be solved. The equations governing the dynamic second-order state can be written as

$$L_{A^*}(\hat{F}^{(2)}) - L_{B^*}(\hat{W}^{(2)}) = -\frac{1}{R}\hat{W}_{,xx}^{(2)} - \hat{W}_{,yy}^{(2)}(\tilde{W}_{,xx}^{(0)} + h\bar{w}_{0,xx}) + \hat{W}_{,xy}^{(1)2} - \hat{W}_{,xx}^{(1)}\hat{W}_{,yy}^{(1)} \tag{22}$$

$$L_{B^*}(\hat{F}^{(2)}) + L_{D^*}(\hat{W}^{(2)}) = \frac{1}{R}\hat{F}_{,xx}^{(2)} + \hat{F}_{,xx}^{(1)}\hat{W}_{,yy}^{(1)} - 2\hat{F}_{,xy}^{(1)}\hat{W}_{,xy}^{(1)} + \hat{F}_{,yy}^{(1)}\hat{W}_{,xx}^{(1)} + \hat{F}_{,xx}^{(0)}\hat{W}_{,yy}^{(2)} - 2\hat{F}_{,xy}^{(0)}\hat{W}_{,xy}^{(2)} + \hat{F}_{,yy}^{(0)}\hat{W}_{,xx}^{(2)} + \hat{F}_{,yy}^{(2)}(\tilde{W}_{,xx}^{(0)} + h\bar{w}_{0,xx}) - \bar{\rho}h\hat{W}_{,tt}^{(2)} + a_d\omega_c^2\bar{\rho}h\hat{W}^{(1)}. \tag{23}$$

These equations admit separable solutions of the form

$$\begin{aligned}\hat{W}^{(2)} = {} & h(W_v^{(20)} + W_t^{(20)}) + h(W_v^{(22)} + W_t^{(22)})\cos 2\omega t \\ & + h\{\hat{w}_{\alpha,20}(x) + \hat{w}_{\beta,20}(x)\cos 2n\theta + \hat{w}_{\gamma,20}(x)\sin 2n\theta\} \\ & + h\{\hat{w}_{\alpha,22}(x) + \hat{w}_{\beta,22}(x)\cos 2n\theta + \hat{w}_{\gamma,22}(x)\sin 2n\theta\}\cos 2\omega t\end{aligned} \tag{24}$$

$$\begin{aligned}\hat{F}^{(2)} = {} & \frac{Eh^2}{cR}\left\{-\frac{1}{2}\lambda^{(20)}y^2 - \bar{\tau}^{(20)}xy\right\} + \frac{Eh^2}{cR}\left\{-\frac{1}{2}\lambda^{(22)}y^2 - \bar{\tau}^{(22)}xy\right\}\cos 2\omega t \\ & + \frac{ERh^2}{c}\{\hat{f}_{\alpha,20}(x) + \hat{f}_{\beta,20}(x)\cos 2n\theta + \hat{f}_{\gamma,20}(x)\sin 2n\theta\} \\ & + \frac{ERh^2}{c}\{\hat{f}_{\alpha,22}(x) + \hat{f}_{\beta,22}(x)\cos 2n\theta + \hat{f}_{\gamma,22}(x)\sin 2n\theta\}\cos 2\omega t.\end{aligned} \tag{25}$$

Details of these equations and the numerical solution procedure can be found in Ref. [17].

The nonlinearity coefficient a_d is equal to zero, and the "dynamic b-factor" b_d becomes [17]

$$b_d = \frac{1}{\omega_c^2 \Delta_d}\{2\hat{F}^{(1)} * (\hat{W}^{(2)}, \hat{W}^{(1)}) + \hat{F}^{(2)} * (\hat{W}^{(1)}, \hat{W}^{(1)})\} \tag{26}$$

where

$$\Delta_d = \int_0^{2\pi}\int_0^{2\pi R}\int_0^{L} \bar{\rho}h\hat{W}^{(1)^2}\,\mathrm{d}x\,\mathrm{d}y\,\mathrm{d}\tau \tag{27}$$

and $\tau = \omega t$, and where the shorthand notation

$$A * (B, C) = \int_0^{2\pi} \int_0^{2\pi R} \int_0^{L} \{A_{,xx}B_{,y}C_{,y} + A_{,yy}B_{,x}C_{,x} - A_{,xy}(B_{,x}C_{,y} + B_{,y}C_{,x})\}\,\mathrm{d}x\,\mathrm{d}y\,\mathrm{d}\tau \tag{28}$$

is used.

5. Results and discussion

The Level-1 Analyses and the Level-2 Analysis have been implemented in FORTRAN programs. The shells that will be used in the numerical calculations are denoted as follows:

Booton's shell: an anisotropic shell used earlier in static stability and vibration investigations [21,14,15]. The data are given in Table 1. For this anisotropic shell, $E = E_{11}$ and $v = v_{12}$ will be used as reference values for Young's modulus and Poisson's ratio, respectively.

ES2-shell: isotropic shell used by Evensen [1]. The vibration mode is characterized by m axial half-waves and ℓ circumferential full waves. The following data are used: $\varepsilon = (\ell^2 h/R)^2 = 0.01$, $\xi = (\pi R/\ell)/(L/m) = 0.1$, $v = 0.3$.

The (normalized) frequency parameters which will be used in the description of the results are given in Table 2.

5.1. Simplified Analysis

The Simplified Analysis is used for parameter studies on a specific laminated shell. The effect of axial loading on the frequency of the mode corresponding to the lowest natural frequency of the perfect shell (''lowest vibration mode'') will be analysed. The shell is subjected to static axial pre-vibration loading $\lambda = \tilde{N}_0/N_{\mathrm{cl}}$, where $N_{\mathrm{cl}} = (Eh^2)/(cR)$, $N_0 = -N_x(x = L)$, and $c = \sqrt{3(1 - v^2)}$, and the quantities $E = E_{11}$ and $v = v_{12}$ are reference values. The variation of the frequency with the loading will be shown up to the load at which the frequency becomes zero.

Table 1
Booton's anisotropic shell

Shell geometry	$R = 67.8$ mm $L = 95.87$ mm
Laminate geometry	3 layers (numbering from outside) $h_1 = h_2 = h_3 = 0.226$ mm $\theta_1 = 30^\circ, \theta_2 = 0^\circ, \theta_3 = -30^\circ$ (Fig. 1)
Layer properties	Glass-epoxy $E_{11} = 4.02 \times 10^4$ MPa $E_{22} = 1.67 \times 10^4$ MPa $v_{12} = 0.363$ $G_{12} = 4.61 \times 10^3$ MPa

Table 2
Normalized frequencies

Ω	$= \omega/\omega_{\mathrm{lin}}$ (Simplified Analysis), ω/ω_c (Extended Analysis).
$\omega/\omega_{m\ell\tau}$	$\omega_{m\ell\tau} = \omega_{\mathrm{lin}}$ evaluated for unloaded perfect shell, Eq. (12).
$\omega/\omega_{\mathrm{ref}}$	$\omega_{\mathrm{ref}} = \frac{E}{2\bar{\rho}R^2}$ ($E = E_{11}$ is a reference value for Young's modulus).
$\bar{\omega}$	$= R\sqrt{(\bar{\rho}h/A_{22})}\,\omega$ (where A_{22} is an element of the ABD-matrix).

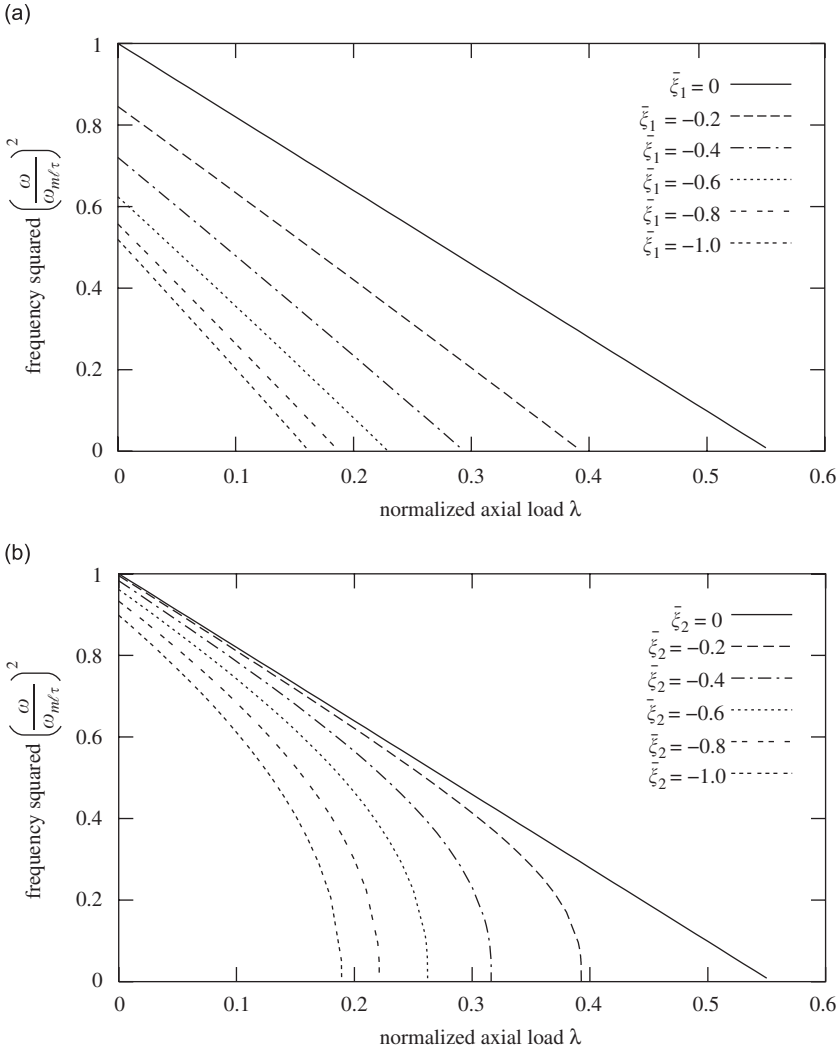

Fig. 2. Influence of axial load on linearized frequency of imperfect anisotropic shell; Booton's shell ($L/R = 1.414$, $R/h = 100$, $\ell = 6$, Table 1), lowest vibration mode: (a) axisymmetric imperfection and (b) asymmetric imperfection. Simplified Analysis.

In Figs. 2a and b the effect of the imperfection amplitude on the load versus frequency curves are given. In Fig. 2a, the curves are plotted for various values of the axisymmetric imperfection amplitude $\bar{\xi}_1$, where

$$\bar{W}/h = \bar{\xi}_1 \cos\frac{2\pi x}{L} \tag{29}$$

and in Fig. 2b for various values of the asymmetric imperfection amplitude $\bar{\xi}_2$, where

$$\bar{W}/h = \bar{\xi}_2 \sin\frac{\pi x}{L}\cos\frac{6}{R}(y - \tau_K x)$$

with $\tau_K = -0.002$. The frequency has been normalized with respect to $\omega_{m\ell\tau}$, the frequency of the unloaded perfect shell of the asymmetric mode considered. The effect of axisymmetric imperfections on the frequency is significant also at zero loading [14]. In the case of asymmetric imperfections, the behaviour becomes strongly nonlinear when the axial load reaches the limit-point load.

In Figs. 3a and b the effect of the vibration amplitude on the load versus frequency curves are given. In Fig. 3a, the curves are plotted for various values of the vibration amplitude for a perfect shell, in Fig. 3b for a shell with a relatively large axisymmetric imperfection. Backbone curves (amplitude–frequency curves) for

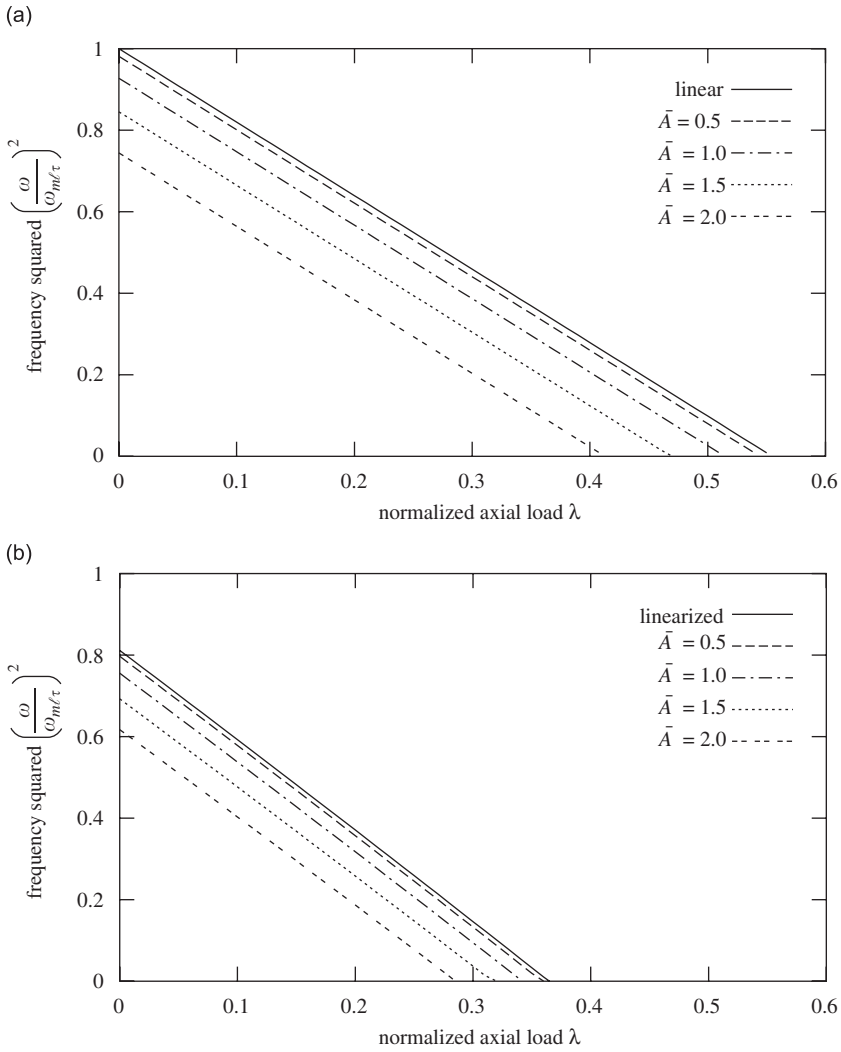

Fig. 3. Influence of axial load on nonlinear frequency of anisotropic shell for finite vibration amplitudes; Booton's shell ($L/R = 1.414$, $R/h = 100$, $\ell = 6$, Table 1), lowest vibration mode: (a) perfect shell, (b) axisymmetric imperfection, $\bar{\xi}_1 = -0.25$. Simplified Analysis.

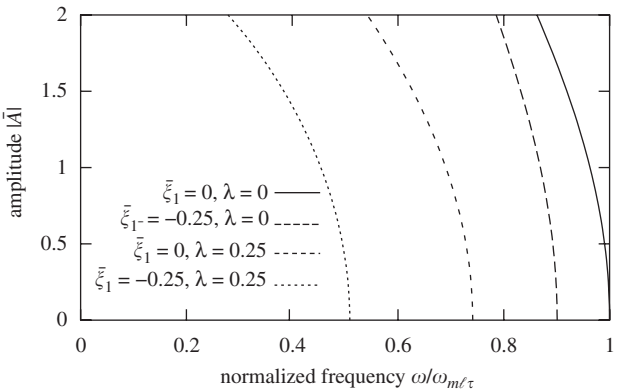

Fig. 4. Backbone curves for axially loaded shell with axisymmetric imperfection; Booton's shell ($L/R = 1.414$, $R/h = 100$, $\ell = 6$, Table 1), lowest vibration mode. Simplified Analysis.

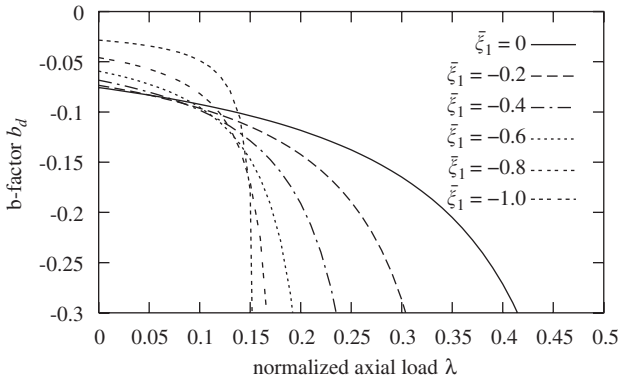

Fig. 5. Influence of axisymmetric imperfection and axial loading on dynamic b-factors of Booton's anisotropic shell ($L/R = 1.414$, $R/h = 100$, $\ell = 6$, Table 1). Simplified Analysis.

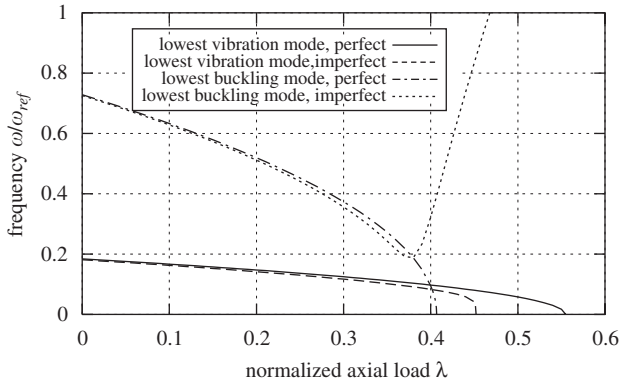

Fig. 6. Effect of axial load on linearized frequency of imperfect Booton's anisotropic shell ($L/R = 1.414$, $R/h = 100$, Table 1) for lowest vibration mode ($\ell = 6$) and lowest buckling mode ($\ell = 5$). Simplified Analysis.

specific values of axial loading ($\lambda = 0$ and 0.25) and axisymmetric imperfection ($\bar{\xi}_1 = 0$ and -0.25) are shown in Fig. 4. The severity of the nonlinearity is conveniently represented by the 'dynamic b-factor' introduced in the Extended Analysis. The dynamic b-factor under axial loading corresponding to the Simplified Analysis is given for Booton's shell with axisymmetric imperfections in Fig. 5, for several values of the imperfection amplitude.

It must be noted that at $\lambda = \lambda_{m\ell\tau} = 0.40691$, the lowest buckling load of this shell occurs for the mode $m = 3$, $\ell = 5$, and $\tau_K = -1.56$ ("lowest buckling mode"), and the frequency corresponding to this mode becomes zero. Above this load level, the static state is unstable. This is illustrated in Fig. 6, where the frequency of the loaded shell is plotted both for the lowest vibration mode and for the lowest buckling mode. The frequency has been normalized with respect to $\omega_{\text{ref}} = E/2\bar{\rho}R^2$, where $E = E_{11}$. Moreover, the effect of an initial imperfection, affine to the vibration or buckling mode, is shown. The imperfection amplitudes used are $\bar{\xi}_1 = -0.04$ and $\bar{\xi}_2 = -0.05$. Note that since the lowest buckling mode has a stable postbuckling behaviour, the frequency of the imperfect shell does not become zero when the load is increased, but it reaches a minimum below the buckling load of the perfect shell and then starts to increase again.

5.2. Extended Analysis

The Simplified Analysis in many cases can reveal the main characteristics of the problem and is suited for parametric studies. The classical "simply supported" boundary conditions ($N_x = v = W = M_x = 0$) are satisfied only approximately in the Simplified Analysis, and the number of modes that is included in the

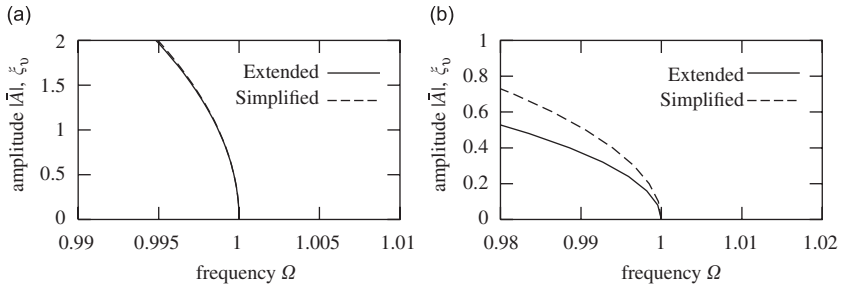

Fig. 7. Backbone curves for perfect shell. b-factors: (a) isotropic shell ES2 ($L/R = 2\pi$, $R/h = 250$, $\ell = 5$) and (b) Booton's anisotropic shell ($L/R = 1.414$, $R/h = 100$, $\ell = 6$, Table 1).

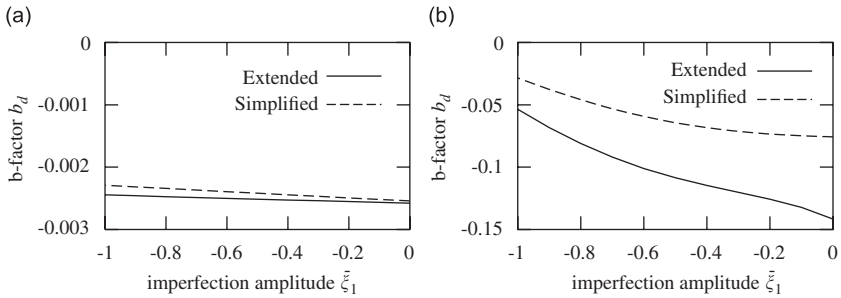

Fig. 8. Influence of axisymmetric imperfection amplitude on dynamic b-factors: (a) isotropic shell ES2 ($L/R = 2\pi$, $R/h = 250$, $\ell = 5$) and (b) Booton's anisotropic shell ($L/R = 1.414$, $R/h = 100$, $\ell = 6$, Table 1).

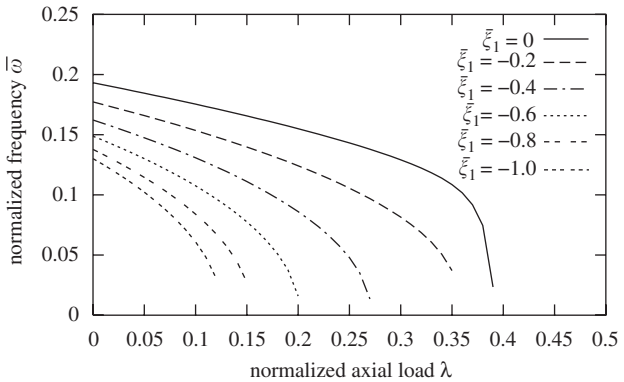

Fig. 9. Influence of axisymmetric imperfection and axial loading on natural frequencies of Booton's anisotropic shell ($L/R = 1.414$, $R/h = 100$, $n = 6$, Table 1). Extended Analysis.

assumed deflection function might not be sufficient. In the Extended Analysis the boundary conditions are satisfied rigorously, the corresponding 'secondary' modes are included, the nonlinear fundamental state is taken into account, and the change of vibration mode during static pre-loading is captured [15].

Backbone curves for a perfect isotropic shell (ES2-shell), and for a perfect anisotropic shell (Booton's shell) are shown in Fig. 7, and in Fig. 8 the dynamic b-factors obtained via the two approaches are shown for the ES2 shell and for Booton's anisotropic shell with an axisymmetric imperfection of the form

$$\bar{W}/h = \bar{\xi}_1 \cos\frac{2\pi x}{L}$$

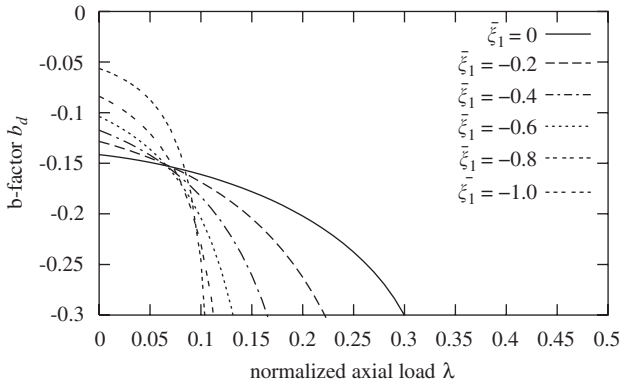

Fig. 10. Influence of axisymmetric imperfection and axial loading on dynamic b-factors of Booton's anisotropic shell ($L/R = 1.414$, $R/h = 100$, $n = 6$, Table 1). Extended Analysis.

In these cases, there is a very good agreement for the ES2 shell, while for Booton's anisotropic shell a larger difference can be observed. For Booton's shell, the double harmonic in the circumferential direction of the shell plays a significant role in the response [13]. For increasing axisymmetric imperfection amplitude (with a negative sign), the nonlinearity becomes less softening, i.e. the dynamic b-factor b_d becomes less negative.

In Fig. 9 the influence of an axisymmetric imperfection and axial loading on the natural frequencies of Booton's anisotropic shell is illustrated. Fig. 10 shows the influence of these factors on the nonlinear behaviour of the shell. A static compressive axial loading has a pronounced effect on the nonlinearity and makes the behaviour more softening. It should be noted that the dynamic b-factor is defined with respect to ω_c, the linearized frequency of the loaded shell with axisymmetric imperfections. The Simplied Analysis (Fig. 5) is able to capture the main trend, but to obtain more accurate results one should use the Extended Analysis.

6. Concluding remarks

In the present paper, the effect of static loading and imperfections on the nonlinear vibration behaviour of cylindrical shells has been studied. Parametric studies have been performed for a specific laminated shell. The strong influence of axial compressive loading and different types of imperfection shapes and amplitudes on the nonlinear vibration behaviour has been shown. For unloaded shells, asymmetric imperfections mainly influence the linearized vibration behaviour, while their effect on the nonlinear vibration behaviour is small. Certain axisymmetric imperfections, satisfying a strong-coupling condition with the asymmetric vibration mode, reduce the linearized vibration frequencies and make the character of the nonlinearity less softening, while the static compressive axial loading makes the nonlinearity more softening.

The two analytical–numerical models (denoted as Level-1 and Level-2 Analysis) that have been used in the present study are typically suitable for initial investigations and parameter studies on the effects of static loading, imperfections, boundary conditions, and geometry and material parameters. They can provide reference solutions for detailed finite element calculations on the vibration behaviour of practical shell structures.

References

[1] D.A. Evensen, Nonlinear flexural vibrations of thin-walled circular cylinders, NASA TN D-4090, 1967.
[2] B.R. El-Zaouk, C.L. Dym, Non-linear vibrations of orthotropic doubly-curved shallow shells, *Journal of Sound and Vibration* 31 (1) (1973) 89–103.
[3] J.C. Chen, Nonlinear Vibrations of Cylindrical Shells, PhD Thesis, California Institute of Technology, Pasadena, California, 1972.
[4] J.H. Ginsberg, Large amplitude forced vibrations of simply supported thin cylindrical shells, *ASME Journal of Applied Mechanics* 40 (1972) 461–477.
[5] M. Ganapathi, T.K. Varadan, Nonlinear free flexural vibrations of laminated circular cylindrical shells, *Composite Structures* 30 (1995) 33–49.

[6] M. Ganapathi, T.K. Varadan, Large amplitude vibrations of circular cylindrical shells, *Journal of Sound and Vibration* 192 (1) (1996) 1–14.
[7] C.M. Chin, A.H. Nayfeh, Bifurcation and chaos in externally excited circular cylindrical shells, *Journal of Applied Mechanics* 63 (1996) 565–574.
[8] F. Pellicano, M. Amabili, M.P. Païdoussis, Effect of the geometry on the non-linear vibration of circular cylindrical shells, *International Journal of Non-Linear Mechanics* 37 (7) (2002) 1181–1198.
[9] E.L. Jansen, A comparison of analytical–numerical models for nonlinear vibrations of cylindrical shells, *Computers & Structures* 82 (2004) 2647–2658.
[10] M. Amabili, Theory and experiments for large-amplitude vibrations of empty and fluid-filled circular cylindrical shell with imperfections, *Journal of Sound and Vibration* 262 (2003) 921–975.
[11] M. Amabili, Nonlinear vibrations of circular cylindrical shells with different boundary conditions, *AIAA Journal* 41 (6) (2003) 119–130.
[12] M. Amabili, M.P. Païdoussis, Review of studies on geometrically nonlinear vibrations and dynamics of circular cylindrical shells and panels, with and without fluid–structure interaction, *Applied Mechanics Review* 56 (4) (2003) 349–381.
[13] E.L. Jansen, A perturbation method for nonlinear vibrations of imperfect structures: application to cylindrical shell vibrations, *International Journal of Solids and Structures* 45 (2008) 1124–1145.
[14] E.L. Jansen, The effect of geometric imperfections on the vibrations of anisotropic cylindrical shells, *Thin-Walled Structures* 45 (2007) 274–282.
[15] E.L. Jansen, Effect of boundary conditions on nonlinear vibration and flutter of laminated cylindrical shells, *Journal of Vibration and Acoustics* 130 (2008) 011003-1–011003-8.
[16] D.A. Evensen, Nonlinear vibration of circular cylindrical shells, in: Y.C. Fung, E.E. Sechler (Eds.), *Thin-Shell Structures—Theory, Experiment and Design*, Prentice-Hall Inc., Englewood Cliffs, NJ, 1974.
[17] E.L. Jansen, Nonlinear Vibrations of Anisotropic Cylindrical Shells, PhD Thesis, Faculty of Aerospace Engineering, Delft University of Technology, The Netherlands, 2001.
[18] U.M. Ascher, R.M.M. Mattheij, R.D. Russell, *Numerical Solution of Boundary Value Problems for Ordinary Differential Equations*, Prentice-Hall Inc., Englewood Cliffs, NJ, 1988.
[19] L.W. Rehfield, Nonlinear free vibrations of elastic structures, *International Journal of Solids and Structures* 9 (1973) 581–590.
[20] J. Wedel-Heinen, Vibrations of geometrically imperfect beam and shell structures, *International Journal of Solids and Structures* 27 (1) (1991) 29–47.
[21] M. Booton, Buckling of imperfect anisotropic cylinders under combined loading, UTIAS Report 203, Institute for Aerospace Studies, University of Toronto, 1976.